

All-Optical Control of the Photonic Hall Lattice in a Pumped Waveguide Array


Shirong Lin^{1,*}, LuoJia Wang,¹ Luqi Yuan^{1,†} and Xianfeng Chen^{1,2,3,4}

¹State Key Laboratory of Advanced Optical Communication Systems and Networks, School of Physics and Astronomy, Shanghai Jiao Tong University, Shanghai 200240, China

²Shanghai Research Center for Quantum Sciences, Shanghai 201315, China

³Jinan Institute of Quantum Technology, Jinan 250101, China

⁴Collaborative Innovation Center of Light Manipulation and Applications, Shandong Normal University, Jinan 250358, China

 (Received 13 January 2022; revised 26 April 2022; accepted 2 May 2022; published 14 June 2022)

The quantum Hall system possesses topologically protected edge states, which have enormous theoretical and practical implications in both fermionic and bosonic systems. Harnessing the quantum Hall effect in optical platforms with lower dimensionality is highly desirable with synthetic dimensions and has attracted broad interests in the photonics society. Here, we introduce an alternative way to realize the artificial magnetic field in a frequency dimension, which is achieved in a pump-probe configuration with cross-phase modulations in a one-dimensional four-waveguide array. The dynamics of the topological chiral edge state has been studied and the influence from the crosstalk of the pump fields has been explored. Our work shows an all-optical way to simulate the quantum Hall system in a photonic system and holds potential applications in manipulating light in waveguide systems.

DOI: [10.1103/PhysRevApplied.17.064029](https://doi.org/10.1103/PhysRevApplied.17.064029)

I. INTRODUCTION

The quantum Hall system, as the well-known topological system, has attracted great attention since its discovery at 1980 [1], and stimulates the flourishing field of topological insulators [2,3]. Simulating the quantum Hall effect in photonics has experienced rapid progress in the past decade, which offers rich potential applications towards generations of optical devices [4–8]. The photonic analog of quantum Hall system has been successfully demonstrated in such various platforms as photonic crystals [9,10], coupled resonator optical waveguides [11,12], polaritonic [13], and optomechanical systems [14]. In particular, the realization of artificial magnetic field [15–18] provides an alternative way to simulate topological photonics systems.

However, it is fundamentally challenging to generate the effective magnetic field in real spaces, and, as alternative ways, there are several methods developed in the synthetic space [19–24]. The concept of synthetic dimension has been widely studied in different optical systems [25–27]. Among these, synthetic dimension based on the frequency axis of light has experienced an increasing amount of investigations [28–34], and turns out to be one of the most promising candidates for emulating topological physics. The original theoretical proposal

in ring resonators utilizes multiple resonant modes connected through dynamic modulation of the refractive index inside the ring [20,21]. On the other hand, nonlinear all-optical techniques have been exploited to achieve one-dimensional frequency dimension either by cross-phase modulation [35–37] or four-wave mixing procedure [28]. These all-optically pumped systems present a fast and efficient approach to manipulating physics in a synthetic dimension. Nevertheless, in realizing the quantum Hall model in all-optically pumped systems with synthetic dimensions might be affected by the crosstalk from separated pump optical fields. Understanding this effect can thus shed light on exploring topological phases in all-optically pumped systems.

Here, we propose a viable all-optical model in a one-dimensional waveguide array to create a photonic quantum Hall system in a synthetic space including the frequency axis of light. In particular, we consider the light propagation inside four coupled waveguides, each of which is driven by a pump laser so a synthetic two-dimensional lattice is configured through cross-phase modulations [38,39]. We then find an alternative implementation of the effective magnetic field based on independently designing the phases of pump laser fields. In this manner, we create a photonic analog of the quantum Hall model. Moreover, we identify the parameters for the crosstalk of pump lasers supporting the chiral edge states and show phase transitions to parameter regions where the topology breaks down. Of note, our scheme not only simulates the

*shironglin@sjtu.edu.cn

†yuanluqi@sjtu.edu.cn

optical counterpart of a nontrivial topological system, but also shows an all-optical way to control the topological system, which could be useful in developing laser-based technologies [40].

II. THEORETICAL MODEL

It has been shown that a probe field propagating inside a single waveguide under the influence of a co-propagating pump can construct the synthetic frequency dimension via cross-phase modulation [35]. We first summarize such behavior here. The evolution of the probe-field amplitude u^s along the z direction can be described by [35,39]

$$\left(i\frac{\partial}{\partial z} + i\Delta\frac{\partial}{\partial t} + V(t)\right)u^s = 0, \quad (1)$$

where Δ represents the group-velocity mismatch between the pump and the probe fields. $V(t) = |u^p(t)|^2$ describes the time-dependent effective potential for the probe field propagating through the waveguide. In deriving Eq. (1), a reference frame where the pump field is at rest has been chosen, which results in the walk-off mismatching parameter Δ , and the probe field is assumed to be weak enough to neglect its self-phase modulation.

Although the shape of the pump field as the writing laser beam can take any form, of most interest to us is the periodical cosine-shape form as $V(t) = P_0(\cos(\Omega t) + 1)$, with P_0 being the peak power of the periodic field and Ω being the modulation frequency, which can be utilized to construct a synthetic lattice structure in the frequency dimension [35]. Therefore, Eq. (1) describes the dynamics of the probe field in a dimension along the frequency axis of light. This fact can be seen if one Fourier transforms Eq. (1) with respect to time as $U^s(\omega) = \int dt u^s(t) \exp(i\omega t)/2\pi$, which yields

$$\left(i\frac{\partial}{\partial z} + \omega\Delta + 2\gamma P_0\right)U^s(\omega) + \gamma P_0[U^s(\omega - \Omega) + U^s(\omega + \Omega)] = 0, \quad (2)$$

where γ denotes the nonlinear coefficient of cross-phase modulation. Furthermore, by the introduction of discrete spectral amplitudes $a_n = U^s(\omega_0 + n\Omega, z) \exp[-i(\omega_0\Delta + 2\kappa)z]$, we obtain [35]

$$\left(i\frac{\partial}{\partial z} + n\Delta\Omega\right)a_n + \kappa(a_{n-1} + a_{n+1}) = 0, \quad (3)$$

where the modulation strength $\kappa \equiv \gamma P_0$. Equation (3) reveals that the spectral component of the probe field at a frequency $\omega_n \equiv \omega_0 + n\Omega$, where ω_0 is a reference frequency and n is an integer, couples to two nearby spectral components at $\omega_0 + (n \pm 1)\Omega$. As such, a synthetic frequency dimension for the probe propagating along z is

constructed utilizing the sideband generation induced by the cross-phase modulation from the pump field.

Based on the all-optical construction of a frequency dimension, we now show that a photonic Hall lattice in a pumped waveguide array can be realized. Light propagation in the synthetic dimensions is illustrated schematically in Fig. 1(a). Our system consists of four waveguides, which form a one-dimensional array. A probe field propagates along the waveguide array under the influence of a co-propagating pump in each waveguide via cross-phase modulations. Under a tight-binding description, the probe field hops between nearest-neighbor waveguides. In such a nonlinear optical system, the evolution of the probe field is described by

$$\left(i\frac{\partial}{\partial z} + i\Delta\frac{\partial}{\partial t} + V_l(t)\right)u_l^s + g(u_{l-1}^s + u_{l+1}^s) = 0, \quad (4)$$

where g is the coupling coefficient of the probe field when it is propagating in the pumped waveguide array, and $l = 1, 2, 3, 4$. Again, applying the same procedure as discussed above, we find that the dynamics of the probe field is given by

$$\left(i\frac{\partial}{\partial z} + n\Delta\Omega\right)a_{n,l} + \kappa(a_{n-1,l} + a_{n+1,l}) + g(a_{n,l-1} + a_{n,l+1}) = 0. \quad (5)$$

In fact, Eq. (5) describes the dynamics of the probe field in synthetic two-dimensional space, which consists of a spatial dimension and a frequency dimension. Hence the equivalence of a two-dimensional lattice shows up.

The strategy to obtain an all-optical equivalent of quantum Hall system in the synthetic dimension is to introduce phase modulation for the individual pump fields. Specifically, for a scheme of $(0, \pi/4, \pi/2, 3\pi/4)$ assigned to the phase of the pump fields in waveguides 1–4 accordingly, we are led to introduce the phase structure of $(0, \pi/2, \pi, 3\pi/2)$ sensed by the probe according to the cross-phase modulations. In Eq. (4), explicitly, we thus have $V_l(t) = P_0(\cos(\Omega t + \phi_l) + 1)$ with $\phi_l = (0, \pi/2, \pi, 3\pi/2)$. Therefore, in a pumped four-waveguide system, the $\pi/2$ phase difference between the neighboring waveguides implements the Landau gauge, and gives rise to a magnetic flux equal to $1/4$ per plaquette [41]. In this way, the equation of motion of the probe field becomes

$$\left(i\frac{\partial}{\partial z} + n\Delta\Omega\right)a_{n,l} + \kappa(a_{n-1,l}e^{i\phi_l} + a_{n+1,l}e^{-i\phi_l}) + g(a_{n,l-1} + a_{n,l+1}) = 0, \quad (6)$$

which corresponds to a charged particle on a square lattice subjected to a magnetic field and an electric field. This is analogous to the Schrödinger equation where the roles

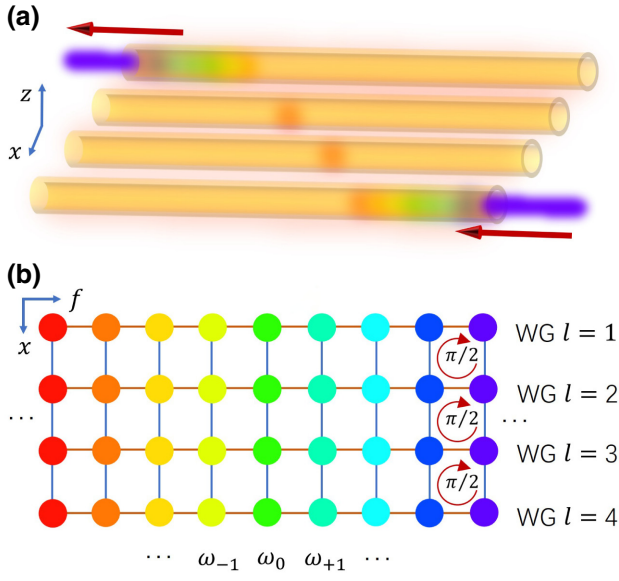


FIG. 1. (a) Schematic of probes propagating in the one-dimensional pumped waveguide array. (b) Synthetic two-dimensional lattice consisting of spatial and frequency dimensions, corresponding to the waveguide array in (a). WG denotes waveguide.

of time, t , are replaced by the propagation direction, z . If the effect resulting from the electric field is negligible, i.e., $n\Delta\Omega \ll \kappa$, we can focus only on the magnetic field, which gives rise to the corresponding Hamiltonian

$$H = \sum_{n,l} \left[\kappa \left(e^{-i\phi_l} a_{n,l}^\dagger a_{n+1,l} + e^{i\phi_l} a_{n+1,l}^\dagger a_{n,l} \right) + g \left(a_{n,l}^\dagger a_{n,l+1} + a_{n,l+1}^\dagger a_{n,l} \right) \right], \quad (7)$$

where $a_{n,l}^\dagger$ ($a_{n,l}$) is the bosonic creation (annihilation) operator. This Hamiltonian informs that the frequency space contributes to one of the dimensions (labeled by the n), as shown in Fig. 1(b). The resulting Hamiltonian is reminiscent of the well-known Hamiltonian of the Harper-Hofstadter model [41,42]. The Harper-Hofstadter model provides the scheme to realize the quantum Hall effect on a lattice in a rational magnetic field $\phi = p/q$ with mutually prime integers p and q , with one exception: $p/q = 1/2$ [43,44]. Hence, in our model, we propose to realize the Harper-Hofstadter model on a square lattice with $\phi = 1/4$, which means that four waveguides can construct the magnetic unit cell. For infinite system or system with periodic boundary condition, the nontrivial topological property of the Harper-Hofstadter model is characterized by the first Chern number (a nontrivial Thouless-Kohmoto-Nightingale-den Nijs (TKNN) invariant) of each band [45]. For a finite system, the topological signature manifests itself in the chiral edge state implied

by the bulk-boundary correspondence [46,47]. Here we consider such a kind of finite system consisting of four waveguides as a minimalist approach, which not only can be used to illustrate the all-optical control of the photonic Hall lattice, but also holds potential feasibility in applications.

We emphasize that, under the all-optical configuration, the crosstalk from separated pump optical fields in nearby waveguides come into play and have a role in the dynamics of the edge states, which therefore requires careful examinations. Following the coupled-mode theory [48–50], we can write the evolution of pump fields along each waveguide with nearest-neighbor couplings

$$i \frac{\partial}{\partial z} u_l^p + g' (u_{l-1}^p + u_{l+1}^p) = 0, \quad (8)$$

where g' represents the coupling coefficient for the pump fields. Consequently, we obtain position-dependent pump power $P_l(z) = |u_l^p(z)|^2$, and thus have a position-dependent modulation strength $\kappa_l(z) \equiv \gamma P_l(z)$, together with the phases $\phi_l(z)$ changing accordingly for the probe field propagating in the l th waveguide. Therefore, the working Hamiltonian depending on propagation distance z becomes

$$H(z) = \sum_{n,l} \left[\kappa_l(z) \left(e^{-i\phi_l(z)} a_{n,l}^\dagger a_{n+1,l} + e^{i\phi_l(z)} a_{n+1,l}^\dagger a_{n,l} \right) + g \left(a_{n,l}^\dagger a_{n,l+1} + a_{n,l+1}^\dagger a_{n,l} \right) \right]. \quad (9)$$

Hamiltonians (7) and (9) are the working equations of our paper, that we use to simulate the quantum Hall-like Hamiltonian (Harper-Hofstadter Hamiltonian) in a synthetic dimension with taking into account the intrinsic pump crosstalk. In view of the inevitable crosstalk of pump fields, we point out that understanding the role of the influence of pump fields in such an all-optical system not only is necessary, but also could provide a flexible way to manipulate light in such photonic Hall lattice.

III. RESULTS AND DISCUSSION

A. Simulation of quantum Hall effects in the synthetic space

As the first demonstration, we begin our numerical analysis by considering the four-waveguide system with independent pump beams. In other words, we ignore the crosstalk between pump fields for the moment so each pump beam affects only the probe field in each waveguide, i.e., $\kappa_l(z) = \kappa_l(0) \equiv \kappa$. In this case, the system is exactly described by Hamiltonian (7). The topological property of this synthetic system manifests itself in the existence of topologically chiral edge states crossing the band gap. By assuming infinite modes along the frequency axis, we

calculate the projected band structure with a Hamiltonian versus k_f , which is reciprocal to the frequency dimension [34]:

$$H_{k_f} = \sum_l \left[2\kappa a_{k_f,l}^\dagger a_{k_f,l} \cos(k_f \Omega_f - \phi_l) + g \left(a_{k_f,l}^\dagger a_{k_f,l+1} + a_{k_f,l+1}^\dagger a_{k_f,l} \right) \right]. \quad (10)$$

The projected band structure is shown in Fig. 2(a). Since we have four waveguides that support a synthetic lattice with four rows [see Fig. 1(b)], four separate bands can be seen in Fig. 2(a). One can see that there is a small gap near the energy ϵ at approximately $1.7g$ and $-1.7g$. This is the result from the large edge-to-bulk ratio given that only four rows are included in the synthetic lattice. Yet, the chiral edge states still exist, of which the field intensity of the states decay exponentially into the bulk [Fig. 2(b)]. One notes that, for an infinite lattice described by Eq. (7) with $\phi_l = (l-1)\pi/2$, the resulting four bands have Chern numbers as 1, -1, -1, 1, respectively, where the middle two bands touch each other at the degenerate points [51,52].

To better study the characteristic of the edge states, we simulate the transport of the wave function of light in a 4×20 synthetic lattice, i.e., only 20 frequency modes are considered in simulations. Artificial boundaries at the frequency dimension are considered. Such a boundary in frequency space can be constructed by engineering the dispersion of the waveguide to create a natural vague boundary [20,29,53]. If the dispersion around considered modes is linear, meaning that the group-velocity dispersion or the higher-order dispersion in the frequency regime of interest can be neglected, the pump-induced coupling is effective and as a result nearby spectral components can be connected without restriction. Nevertheless, if near a particular spectral mode, the dispersion relation becomes largely nonlinear, the coupling between this particular spectral mode and another nearby mode become inefficient, failing to connect two synthetic sites. Following this sense, this particular mode gives an artificial boundary in the frequency axis [20]. Another possibility is to use the atom at a transition frequency resonant with a target spectral mode in waveguides, so the frequency near such a mode experiences large dispersion due to the resonant energy splitting [54].

We write the wave function of light as [34]

$$|\Psi(z)\rangle = \sum_{n,l} v_{n,l} a_{n,l}^\dagger |0\rangle, \quad (11)$$

in which $v_{n,l}$ is the probability amplitude of the photon state at site (n,l) . By substituting Eq. (11) into the Schrödinger-like equation $id|\Psi(z)\rangle/dz = H|\Psi(z)\rangle$, we

find the governing working equation is

$$\frac{d}{dz} v_{n,l} = -ik \left(v_{n+1,l} e^{-i\phi_l} + v_{n-1,l} e^{i\phi_l} \right) - ig \left(v_{n,l+1} + v_{n,l-1} \right) + s \delta_{n,1} \delta_{l,1}. \quad (12)$$

Note that to excite the system, a source excitation $s = e^{-i\Delta kz}$ has been adopted, which is applied to excite the 11th frequency mode in the first waveguide. Here, Δk is the wavevector mismatching with respect to that of the considered mode [54], and such an excitation can be achieved by using the traveling excitation field propagating inside an additional waveguide weakly coupled to the first waveguide of the system [55]. In Fig. 2(c), we show the calculated distribution of the intensity $|v_{n,l}|^2$ in the synthetic lattice at the propagation distance $z = 40g^{-1}$. One can see a one-way propagation of the edge state in the synthetic space, i.e., the edge state propagates unidirectionally along the boundaries of the synthetic lattice. It is instructive to investigate the average intensity spectra, $I_{n,l} \equiv \int |v_{n,l}|^2 dz$. The values of $|v_{n,l}|^2$ are related to the number of photons at each lattice site (n,l) , and therefore $I_{n,l}$ gives the average intensity spectra for the probe field propagating through each entire waveguide, which is plotted in Fig. 2(d). Our results here show that the energy of the probe is confined on the boundary of the synthetic lattice and cannot diffuse into the bulk in the pumped waveguide system. It turns out that by all-optically controlling the phase pattern of the pump fields, we can manipulate the photonic lattice, enabling a transition from trivial to topological regime (see Parts S1 and S2 within the Supplemental Material [56]).

B. Coupled-mode analysis on the crosstalk of pump fields

To explore the role of the crosstalk between pumps, we now perform the analysis based on the coupled-mode theory [48–50] to study the interactions of pump fields in different waveguides. In particular, we numerically solve Eq. (8) with initial conditions $[u_1^p(0), u_2^p(0), u_3^p(0), u_4^p(0)] = u_0[1, \exp(i\pi/4), \exp(i\pi/2), \exp(3i\pi/4)]$. This initial condition for pumps indicates that four waveguides are pumped by optical fields at the same intensity but different phases, which is exactly what we use in the previous subsection. However, here, we consider changes of pumps propagating through waveguides due to the crosstalk. We take two examples under different coupling coefficients for the pumps: $g'/g = 0.001$ and $g'/g = 0.01$. In Fig. 3, we plot the simulation results of powers $P_l(z)$ and the resulting phases $\phi_l(z) = 2\text{Arg}[u_l^p(z)]$ of pumps in each waveguide versus the propagating distance z .

Figure 3(a) clearly shows that powers P_l become position dependent for $g'/g = 0.001$. The pump powers in waveguides 1 and 2 decrease from their initial values

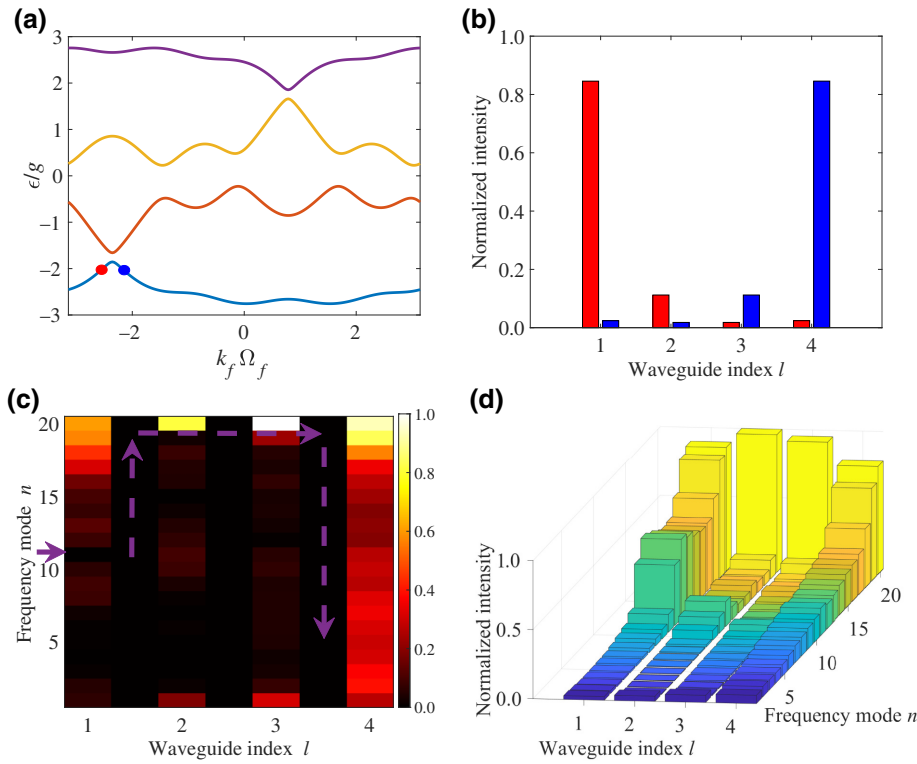


FIG. 2. (a) Projected band structure versus k_f for the four-waveguide system. (b) Field intensity distributions of the two edge states indicated by red and blue dots in (a), which are localized on the two boundaries and decay exponentially into the bulk. (c) Distribution of $|v_{n,l}|^2$ in simulation in a 4×20 lattice, with the initial excitation source being $s = e^{-i\Delta k z}$ with $\Delta k = -2g$ applied in the 11th mode of waveguide 1 denoted by the arrow, to excite the exact edge state with a red dot in (a). The unidirectionally propagating chiral edge state is indicated by dashed purple arrows. Depicted is the field profile at $z = 40g^{-1}$. (d) The average intensity spectra $I_{n,l}$ for the probe field at each waveguide.

$P_{1,2}(0) = |u_0|^2$ in the simulation range of $gz \in [0, 60]$. At the same time, the pump powers in waveguides 3 and 4 increase. Notice that as compared with the changes of the pump powers in waveguides 1 and 4, those in waveguides 2 and 3 change more slowly, which can be seen in the inset of Fig. 3(a). The reason is that the initial phases play a significant role in the redistribution of energy in the waveguide array through the interference among the amplitudes of the pumps. Compared with the case of the simulation with initially no phase difference, the pump field in waveguide 1(2) changes equivalently to that in waveguide 4(3). However, for the case with initial phase difference, such degeneracy due to the symmetry is lifted as shown in Fig. 3(a). As the

coupling coefficient increases, such as $g'/g = 0.01$, the impact of the crosstalk gets larger, which is illustrated in Fig. 3(c).

The crosstalk of the pump fields not only affects the power redistributions, but more is more, it brings disorder into the phase distribution of the pump field inside each waveguide, as plotted in Figs. 3(b) and 3(d). Comparing the results with different amplitudes of g' in Figs. 3(b) and 3(d), one can see that for the weak coupling case $g'/g = 0.001$, the phases for pump fields in each waveguide experience a small linear change in the propagation range of $gz = 60$. Moreover, phases in waveguides 1 and 4 change more slowly than those in waveguides 2 and 3. As the coupling coefficient of the pump

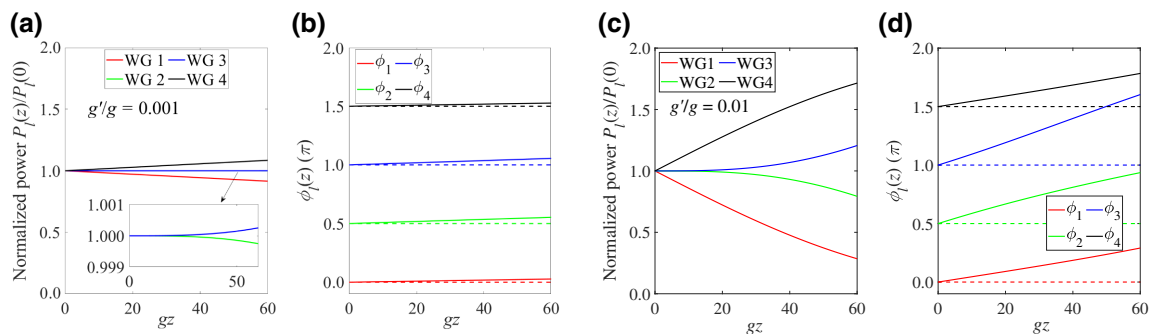


FIG. 3. Simulation results of powers $P_l(z)$ and the resulting phases $\phi_l(z) = 2\text{Arg}[u_l^p(z)]$ of pumps in each waveguide (WG). (a),(b) $g'/g = 0.001$; (c),(d) $g'/g = 0.01$.

fields increases, all phases have been changed dramatically within the same propagation distance. Therefore, the coupled-mode analysis explicitly shows that the evolution of the powers and phases of the pump fields depends on both the coupling coefficient g' and the propagation distance z , which shall affect the dynamics of edge states for the probe field.

C. All-optical control of edge states

We are now in a position to take the coupled-mode results for the pump fields into account and explore its effect on the probe propagation. The fundamental difference between the Hamiltonian with the coupled pump fields in Eq. (9) and Hamiltonian (7) that we study in Sec. III A is that hopping coefficients for the probe field $\kappa_l(z)$ and phases $\phi_l(z)$ in the l th waveguide is no longer uniform and identical, which are dependent on the pump field $u_l^p(z)$ in the array.

Firstly, we study the small coupling case, i.e., $g'/g = 0.001$. We perform simulations with Hamiltonian (9) using the same parameters as those for Figs. 2(c) and 2(d), and plot results in Figs. 4(a)–4(c). Figure 4(a) plots the distribution of the intensity $|v_{n,l}|^2$ in the synthetic lattice at the propagation distance $z = 40g^{-1}$. Due to the crosstalk between the pump fields in different waveguides, it shows small deviation from the results in Fig. 2(c) where the crosstalk is ignored. This small difference in two cases can also be seen from the average intensity spectra $I_{n,l}$ plotted in Fig. 4(b), which shows that the most part of the energy of the probe field is confined to the boundary of the synthetic lattice. To better explore the energy distribution, the boundary region and the bulk region of the synthetic lattice structure are separated, and the average intensity distributed in the boundary and the bulk sites are defined by I_{boundary} and I_{bulk} , respectively. Specifically, the boundary region corresponds to all the frequency modes in waveguides 1 and 4, as well as the highest and lowest frequency modes in waveguides 2 and 3, while the rest modes in waveguides 2 and 3 contribute to the bulk region. Hence, following this specific separation rule we can define $I_{\text{boundary}} = I_{\text{boundary}}^{\text{WG1}} + I_{\text{boundary}}^{\text{WG2}} + I_{\text{boundary}}^{\text{WG3}} + I_{\text{boundary}}^{\text{WG4}}$, and $I_{\text{bulk}} = I_{\text{bulk}}^{\text{WG2}} + I_{\text{bulk}}^{\text{WG3}}$, where the distribution of the average intensity inside each part is depicted in Fig. 4(c). One can see that the boundary part I_{boundary} contributes about 88% of the total energy in which the frequency modes in waveguide 1 ($I_{\text{boundary}}^{\text{WG1}}$) account for more than half of the energy of the edge state, whereas the bulk part I_{bulk} occupies approximately 12% of the total energy. We thus find that the probe field exhibits its edge state under the influence of a small crosstalk effect ($g'/g = 0.001$) from the pump fields.

Secondly, we consider the case with the significant coupling coefficient for the pump fields, e.g., $g'/g = 0.01$. Figure 4(d) shows the intensity $|v_{n,l}|^2$ of the probe field

at the propagation distance $z = 40g^{-1}$. One finds that, at this distance, the probe field propagates into the bulk region dramatically. More specifically, the energy distribution in the synthetic lattice tends to confine to all frequency modes in waveguide 1 and waveguide 2. Figure 4(e) plots the average intensity spectra $I_{n,l}$, which confirms this tendency. In Fig. 4(f), we show the distribution of average intensity inside each part we define in the previous paragraph, where we find that the coupling coefficient for the pump fields clearly redistributes energy in the boundary region and the bulk region. By comparing the case with $g'/g = 0.001$, we find that more energy is diverted from boundary parts to bulk parts, resulting approximately 25% in the bulk region. The result in the case with $g'/g = 0.01$, as shown in Fig. 4(e), however, is that the probe field gets the unidirectional frequency conversion and obtains the peak power in the vicinity of the frequency mode $n = 15$ in waveguide 1, while the energy of the probe penetrates into the bulk near the 15th mode in waveguide 2. Such a phenomenon comes from the competition between the topological effect and the disorder in the modulation strengths and the phases for the probe due to the crosstalk from the pump fields.

To illustrate the influence of the crosstalk from the pump fields in this all-optical configuration in more details, we present the results of the numerically calculated ratio of the average intensity of the frequency modes in the bulk region to those in the boundary region, i.e., $I_{\text{bulk}}/I_{\text{boundary}}$, as a function of the propagation distance and the coupling coefficient for the pump fields, g' , as shown in Fig. 4(g). It serves as a quantitative indicator to investigate the edge-mode dynamics. More specifically, when the value of $I_{\text{bulk}}/I_{\text{boundary}}$ is smaller (larger) than 1, it represents that the boundary (bulk) modes dominates at the parameter space (z, g') . This phase diagram in Fig. 4(g) shows that there exhibits edge state for small g' or short propagation distance. In such a parameter space, I_{boundary} changes continuously. However, in the region that $I_{\text{bulk}}/I_{\text{boundary}} > 1$, this ratio undergoes oscillations in the parameter space with large g' and long propagation distance. We examine such behavior of the ratio $I_{\text{bulk}}/I_{\text{boundary}}$ with different choices of g' in Fig. 4(h). One can see that, for $g' = 0$, the propagating modes of the probe field on the boundary of the synthetic lattice overwhelmingly dominates. In the case with $g'/g = 0.001$, similar behavior can be seen with small deviation. As the value of g'/g increases, more energy is transferred from the boundary region to the bulk region during the probe propagates. While it is still the edge-mode dominates for the case with $g'/g = 0.01$ in the propagation range $gz = 60$, in the case with $g'/g = 0.03$ the ratio $I_{\text{bulk}}/I_{\text{boundary}}$ transit quickly to the bulk-mode dominated region and oscillates with z from the reflection at boundaries in the synthetic lattice. In this case, due to the relatively large crosstalk between the pump fields in different waveguides during the propagation, the chiral

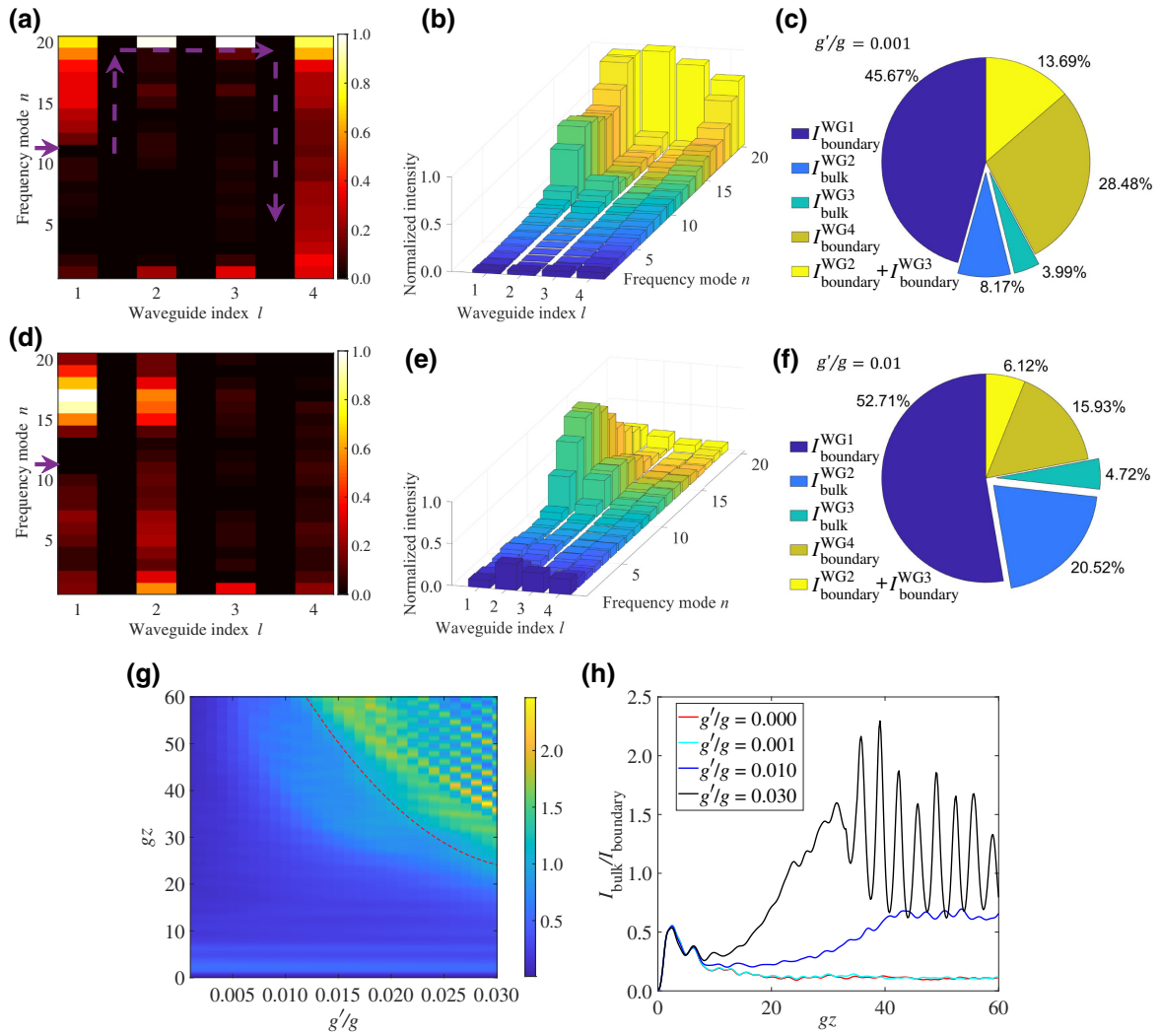


FIG. 4. Simulation results in two cases with $g'/g = 0.001$ (a)–(c), and with $g'/g = 0.01$ (d)–(f), under the same excitation as discussed in Fig. 2. (a),(d) Distributions of $|v_{n,l}|^2$ for the probe field at $z = 40g^{-1}$. (b),(e) Average intensity spectra $I_{n,l}$ for the probe field at each waveguide. (c),(f) Distributions of the energy in different bulk and boundary parts. (g) Phase diagram of $I_{\text{bulk}}/I_{\text{boundary}}$ as a function of the propagation distance and the coupling coefficient for the pump fields. Red dashed line denotes $I_{\text{bulk}}/I_{\text{boundary}} \sim 1$. (h) Plots of $I_{\text{bulk}}/I_{\text{boundary}}$ as a function of the propagation distance for cases with $g'/g = 0, 0.001, 0.01, 0.03$.

edge state cannot be maintained, making the quantum Hall phase breakdown.

Our study can be further generalized to a larger system, e.g., using ten pumped waveguides, where much smaller edge-to-bulk ratio can be reached (see the Supplemental Material for details [56]). We further note that our results show only moderate protection from the pump crosstalk in our proposed model, which indicates that the crosstalk between different pumps indeed brings substantial effect on the synthetic Hall lattice here. However, from a practical point of view, it is useful to see the influence of the pump crosstalk, and the resulting phase diagram in Fig. 4(g) can be helpful for finding the suitable pump parameter and propagation distance for further designing the topological device.

IV. DISCUSSION AND CONCLUSION

Experimentally, the synthetic frequency axis of light via cross-phase modulation has been observed in an optical fiber system [36,37]. The demonstration of our theoretical proposal consisting of a frequency dimension and a spatial dimension requires an array of coupled waveguides, which can be fabricated using the optical induction technique [57,58] or the femtosecond laser direct-writing technique [59,60]. To ignore the effective electric field in the synthetic two-dimensional lattice, it needs the condition that $\gamma P_0 \gg n\Delta\Omega$, which can be matched by either choosing materials with large optical nonlinearity or high pump power, or considering a small walk-off parameter or modulation frequency. On the other hand, in order to control the

crosstalk from the pump optical fields, one can vary the wavelength of the pump fields so that the coupling coefficient of the pump fields in the waveguide array changes accordingly [61–64]. Hence, the desired wavelength window allows one to tune the ratio of coupling coefficients g'/g . Moreover, there are several alternative experimental approaches, which have been demonstrated to be able to control the crosstalk in waveguide systems, such as examples of using transformation optics [65], anisotropic metamaterials [66], and methods inspired from the atomic physics [67,68]. Therefore, it is possible to construct the two-dimensional synthetic lattice in a waveguide array and control the crosstalk in such a platform under the current photonic technology, making our proposal feasible to be experimentally realized.

In summary, we study the light transport in a quantum Hall system in the synthetic space, consisting of the probe field propagating in a one-dimensional four-waveguide array driven by pump fields at the designed phase distribution. The interaction between the pump and probe field via cross-phase modulations inside each waveguide induces a synthetic frequency dimension, and moreover, the phase distribution of the pump fields provides an alternative all-optical path towards the realization of artificial gauge potential and hence effective magnetic field for photons in the pumped waveguide array. We explore the dynamics of the topological chiral edge states and also the edge-mode dynamics affected by the crosstalk of pump lasers, where the parameter space is investigated to seek potential controllability of the probe flow in the synthetic space. Besides the four-waveguide system, our study can also be generalized to a system with a larger number of waveguides and to higher-dimensional waveguide arrays. Our work focuses on the impact of the pump crosstalk on the robustness of topological properties in a synthetic photonic Hall system, which could pave the way for designing potential topological photonic devices. The all-optically control of chiral transport of light on the boundary in a synthetic space can be of great significance in nonlinear frequency generation and signal multiplexing for communication [40].

Note.—Related to and independent of our work, a recent paper [69] has proposed topological frequency control of broadband signals in modulated waveguided arrays.

ACKNOWLEDGMENTS

The research is supported by National Natural Science Foundation of China (Grants No. 12122407, No. 11974245, and No. 12104296), National Key R&D Program of China (Grant No. 2017YFA0303701), Shanghai Municipal Science and Technology Major Project (Grant No. 2019SHZDZX01), Natural Science Foundation of Shanghai (Grant No. 19ZR1475700). L.Y. acknowledges the support from the Program for Professor of Special Appointment (Eastern Scholar) at Shanghai Institutions

of Higher Learning. X.C. also acknowledges the support from Shandong Quancheng Scholarship (Grant No. 00242019024).

-
- [1] K. v. Klitzing, G. Dorda, and M. Pepper, New Method for High-Accuracy Determination of the Fine-Structure Constant Based on Quantized Hall Resistance, *Phys. Rev. Lett.* **45**, 494 (1980).
 - [2] D. Xiao, M.-C. Chang, and Q. Niu, Berry phase effects on electronic properties, *Rev. Mod. Phys.* **82**, 1959 (2010).
 - [3] Y. Ren, Z. Qiao, and Q. Niu, Topological phases in two-dimensional materials: A review, *Rep. Prog. Phys.* **79**, 066501 (2016).
 - [4] X.-C. Sun, C. He, X.-P. Liu, M.-H. Lu, S.-N. Zhu, and Y.-F. Chen, Two-dimensional topological photonic systems, *Prog. Quantum Electron.* **55**, 52 (2017).
 - [5] A. B. Khanikaev and G. Shvets, Two-dimensional topological photonics, *Nat. Photon.* **11**, 763 (2017).
 - [6] T. Ozawa, H. M. Price, A. Amo, N. Goldman, M. Hafezi, L. Lu, M. C. Rechtsman, D. Schuster, J. Simon, and O. Zeitlinger, *et al.*, Topological photonics, *Rev. Mod. Phys.* **91**, 015006 (2019).
 - [7] Y. Wu, C. Li, X. Hu, Y. Ao, Y. Zhao, and Q. Gong, Applications of topological photonics in integrated photonic devices, *Adv. Opt. Mater.* **5**, 1700357 (2017).
 - [8] M. Kremer, L. J. Maczewsky, M. Heinrich, and A. Szameit, Topological effects in integrated photonic waveguide structures, *Opt. Mater. Express* **11**, 1014 (2021).
 - [9] F. Haldane and S. Raghu, Possible Realization of Directional Optical Waveguides in Photonic Crystals with Broken Time-Reversal Symmetry, *Phys. Rev. Lett.* **100**, 013904 (2008).
 - [10] Z. Wang, Y. Chong, J. D. Joannopoulos, and M. Soljačić, Reflection-free One-Way Edge Modes in a Gyromagnetic Photonic Crystal, *Phys. Rev. Lett.* **100**, 013905 (2008).
 - [11] M. Hafezi, S. Mittal, J. Fan, A. Migdall, and J. Taylor, Imaging topological edge states in silicon photonics, *Nat. Photon.* **7**, 1001 (2013).
 - [12] S. Mittal, S. Ganeshan, J. Fan, A. Vaezi, and M. Hafezi, Measurement of topological invariants in a 2D photonic system, *Nat. Photon.* **10**, 180 (2016).
 - [13] T. Karzig, C.-E. Bardyn, N. H. Lindner, and G. Refael, Topological Polaritons, *Phys. Rev. X* **5**, 031001 (2015).
 - [14] M. Schmidt, S. Kessler, V. Peano, O. Painter, and F. Marquardt, Optomechanical creation of magnetic fields for photons on a lattice, *Optica* **2**, 635 (2015).
 - [15] K. Fang, Z. Yu, and S. Fan, Realizing effective magnetic field for photons by controlling the phase of dynamic modulation, *Nat. Photon.* **6**, 782 (2012).
 - [16] K. Fang, Z. Yu, and S. Fan, Photonic Aharonov-Bohm Effect Based on Dynamic Modulation, *Phys. Rev. Lett.* **108**, 153901 (2012).
 - [17] K. Fang, Z. Yu, and S. Fan, Experimental demonstration of a photonic Aharonov-Bohm effect at radio frequencies, *Phys. Rev. B* **87**, 060301(R) (2013).
 - [18] L. D. Tzuang, K. Fang, P. Nussenzeig, S. Fan, and M. Lipson, Non-reciprocal phase shift induced by an effective magnetic flux for light, *Nat. Photon.* **8**, 701 (2014).

- [19] X.-W. Luo, X. Zhou, C.-F. Li, J.-S. Xu, G.-C. Guo, and Z.-W. Zhou, Quantum simulation of 2D topological physics in a 1D array of optical cavities, *Nat. Commun.* **6**, 1 (2015).
- [20] L. Yuan, Y. Shi, and S. Fan, Photonic gauge potential in a system with a synthetic frequency dimension, *Opt. Lett.* **41**, 741 (2016).
- [21] T. Ozawa, H. M. Price, N. Goldman, O. Zilberberg, and I. Carusotto, Synthetic dimensions in integrated photonics: From optical isolation to four-dimensional quantum hall physics, *Phys. Rev. A* **93**, 043827 (2016).
- [22] E. Lustig, S. Weimann, Y. Plotnik, Y. Lumer, M. A. Bandres, A. Szameit, and M. Segev, Photonic topological insulator in synthetic dimensions, *Nature* **567**, 356 (2019).
- [23] A. Dutt, Q. Lin, L. Yuan, M. Minkov, M. Xiao, and S. Fan, A single photonic cavity with two independent physical synthetic dimensions, *Science* **367**, 59 (2020).
- [24] C. Leefmans, A. Dutt, J. Williams, L. Yuan, M. Parto, F. Nori, S. Fan, and A. Marandi, Topological dissipation in a time-multiplexed photonic resonator network, *Nat. Phys.*, 1 (2022).
- [25] L. Yuan, Q. Lin, M. Xiao, and S. Fan, Synthetic dimension in photonics, *Optica* **5**, 1396 (2018).
- [26] T. Ozawa and H. M. Price, Topological quantum matter in synthetic dimensions, *Nat. Rev. Phys.* **1**, 349 (2019).
- [27] E. Lustig and M. Segev, Topological photonics in synthetic dimensions, *Adv. Opt. Photon.* **13**, 426 (2021).
- [28] B. A. Bell, K. Wang, A. S. Solntsev, D. N. Neshev, A. A. Sukhorukov, and B. J. Eggleton, Spectral photonic lattices with complex long-range coupling, *Optica* **4**, 1433 (2017).
- [29] C. Qin, F. Zhou, Y. Peng, D. Sounas, X. Zhu, B. Wang, J. Dong, X. Zhang, A. Alù, and P. Lu, Spectrum Control through Discrete Frequency Diffraction in the Presence of Photonic Gauge Potentials, *Phys. Rev. Lett.* **120**, 133901 (2018).
- [30] A. Dutt, M. Minkov, Q. Lin, L. Yuan, D. A. Miller, and S. Fan, Experimental band structure spectroscopy along a synthetic dimension, *Nat. Commun.* **10**, 1 (2019).
- [31] G. Li, Y. Zheng, A. Dutt, D. Yu, Q. Shan, S. Liu, L. Yuan, S. Fan, and X. Chen, Dynamic band structure measurement in the synthetic space, *Sci. Adv.* **7**, eabe4335 (2021).
- [32] H. Chen, N. Yang, C. Qin, W. Li, B. Wang, T. Han, C. Zhang, W. Liu, K. Wang, and H. Long, *et al.*, Real-time observation of frequency Bloch oscillations with fibre loop modulation, *Light: Sci. Appl.* **10**, 1 (2021).
- [33] K. Wang, A. Dutt, K. Y. Yang, C. C. Wojcik, J. Vučković, and S. Fan, Generating arbitrary topological windings of a non-Hermitian band, *Science* **371**, 1240 (2021).
- [34] L. Yuan, A. Dutt, and S. Fan, Synthetic frequency dimensions in dynamically modulated ring, *APL Photon.* **6**, 071102 (2021).
- [35] U. Peschel, C. Bersch, and G. Onishchukov, Discreteness in time, *Open Phys.* **6**, 619 (2008).
- [36] C. Bersch, G. Onishchukov, and U. Peschel, Experimental observation of spectral Bloch oscillations, *Opt. Lett.* **34**, 2372 (2009).
- [37] C. Bersch, G. Onishchukov, and U. Peschel, Spectral and temporal Bloch oscillations in optical fibres, *Appl. Phys. B* **104**, 495 (2011).
- [38] Q. Lin, O. J. Painter, and G. P. Agrawal, Nonlinear optical phenomena in silicon waveguides: Modeling and applications, *Opt. Express* **15**, 16604 (2007).
- [39] G. Agrawal, *Nonlinear Fiber Optics* (Academic, New York, 2007), 4th ed.
- [40] Z. Chen and M. Segev, Highlighting photonics: Looking into the next decade, *eLight* **1**, 1 (2021).
- [41] D. R. Hofstadter, Energy levels and wave functions of Bloch electrons in rational and irrational magnetic fields, *Phys. Rev. B* **14**, 2239 (1976).
- [42] P. G. Harper, Single band motion of conduction electrons in a uniform magnetic field, *Proc. Phys. Soc. Sec. A* **68**, 874 (1955).
- [43] Y. Hatsugai and M. Kohmoto, Energy spectrum and the quantum Hall effect on the square lattice with next-nearest-neighbor hopping, *Phys. Rev. B* **42**, 8282 (1990).
- [44] I. I. Satija, *The Butterfly in the Quantum World: The Story of the Most Fascinating Quantum Fractal* (Morgan & Claypool Publishers, San Rafael, CA, 2016).
- [45] D. J. Thouless, M. Kohmoto, M. P. Nightingale, and M. den Nijs, Quantized Hall Conductance in a Two-Dimensional Periodic Potential, *Phys. Rev. Lett.* **49**, 405 (1982).
- [46] Y. Hatsugai, Chern Number and Edge States in the Integer Quantum Hall Effect, *Phys. Rev. Lett.* **71**, 3697 (1993).
- [47] M. Z. Hasan and C. L. Kane, Colloquium: Topological insulators, *Rev. Mod. Phys.* **82**, 3045 (2010).
- [48] A. Yariv, Coupled-mode theory for guided-wave optics, *IEEE J. Quantum Electron.* **9**, 919 (1973).
- [49] H. A. Haus and W. Huang, Coupled-mode theory, *Proc. IEEE* **79**, 1505 (1991).
- [50] W.-P. Huang, Coupled-mode theory for optical waveguides: An overview, *J. Opt. Soc. Am. A* **11**, 963 (1994).
- [51] M. Kohmoto, Zero modes and the quantized Hall conductance of the two-dimensional lattice in a magnetic field, *Phys. Rev. B* **39**, 11943 (1989).
- [52] M. Aidelsburger, M. Lohse, C. Schweizer, M. Atala, J. T. Barreiro, S. Nascimbène, N. Cooper, I. Bloch, and N. Goldman, Measuring the Chern number of Hofstadter bands with ultracold bosonic atoms, *Nat. Phys.* **11**, 162 (2015).
- [53] Q. Shan, D. Yu, G. Li, L. Yuan, and X. Chen, One-way topological states along vague boundaries in synthetic frequency dimensions including group velocity dispersion, *Prog. Electromagn. Res.* **169**, 33 (2020).
- [54] L. Yuan, D.-w. Wang, and S. Fan, Synthetic gauge potential and effective magnetic field in a Raman medium undergoing molecular modulation, *Phys. Rev. A* **95**, 033801 (2017).
- [55] S. Stützer, Y. Plotnik, Y. Lumer, P. Titum, N. H. Lindner, M. Segev, M. C. Rechtsman, and A. Szameit, Photonic topological anderson insulators, *Nature* **560**, 461 (2018).
- [56] See Supplemental Material at <http://link.aps.org/supplemental/10.1103/PhysRevApplied.17.064029> for simulation results of light propagation in the topologically trivial counterparts without (Sec. S1) and with (Sec. S2) crosstalk of the pump fields, and a discussion of edge-mode dynamics in a system with much smaller edge-to-bulk ratio by using ten pumped waveguides (Sec. S3).
- [57] N. K. Efremidis, S. Sears, D. N. Christodoulides, J. W. Fleischer, and M. Segev, Discrete solitons in photorefractive optically induced photonic lattices, *Phys. Rev. E* **66**, 046602 (2002).
- [58] J. W. Fleischer, M. Segev, N. K. Efremidis, and D. N. Christodoulides, Observation of two-dimensional discrete

- solitons in optically induced nonlinear photonic lattices, *Nature* **422**, 147 (2003).
- [59] A. Szameit, D. Blömer, J. Burghoff, T. Schreiber, T. Pertsch, S. Nolte, A. Tünnermann, and F. Lederer, Discrete nonlinear localization in femtosecond laser written waveguides in fused silica, *Opt. Express* **13**, 10552 (2005).
- [60] A. Szameit, J. Burghoff, T. Pertsch, S. Nolte, A. Tünnermann, and F. Lederer, Two-dimensional soliton in cubic fs laser written waveguide arrays in fused silica, *Opt. Express* **14**, 6055 (2006).
- [61] R. Iwanow, D. A. May-Arrijoja, D. N. Christodoulides, G. I. Stegeman, Y. Min, and W. Sohler, Discrete Talbot Effect in Waveguide Arrays, *Phys. Rev. Lett.* **95**, 053902 (2005).
- [62] A. S. Solntsev, A. A. Sukhorukov, D. N. Neshev, and Y. S. Kivshar, Spontaneous Parametric Down-Conversion and Quantum Walks in Arrays of Quadratic Nonlinear Waveguides, *Phys. Rev. Lett.* **108**, 023601 (2012).
- [63] S. Yu, X. Piao, D. R. Mason, S. In, and N. Park, Spatiospectral separation of exceptional points in PT -symmetric optical potentials, *Phys. Rev. A* **86**, 031802(R) (2012).
- [64] R. Kruse, F. Katzschmann, A. Christ, A. Schreiber, S. Wilhelm, K. Laiho, A. Gábris, C. S. Hamilton, I. Jex, and C. Silberhorn, Spatio-spectral characteristics of parametric down-conversion in waveguide arrays, *New J. Phys.* **15**, 083046 (2013).
- [65] L. H. Gabrielli, D. Liu, S. G. Johnson, and M. Lipson, On-chip transformation optics for multimode waveguide bends, *Nat. Commun.* **3**, 1 (2012).
- [66] S. Jahani, S. Kim, J. Atkinson, J. C. Wirth, F. Kalhor, A. Al Noman, W. D. Newman, P. Shekhar, K. Han, and V. Van, *et al.*, Controlling evanescent waves using silicon photonic all-dielectric metamaterials for dense integration, *Nat. Commun.* **9**, 1 (2018).
- [67] W. Song, R. Gatlula, S. Abbaslou, M. Lu, A. Stein, W. Y. Lai, J. Provine, R. F. W. Pease, D. N. Christodoulides, and W. Jiang, High-density waveguide superlattices with low crosstalk, *Nat. Commun.* **6**, 1 (2015).
- [68] M. Mrejen, H. Suchowski, T. Hatakeyama, C. Wu, L. Feng, K. O'Brien, Y. Wang, and X. Zhang, Adiabatic elimination-based coupling control in densely packed subwavelength waveguides, *Nat. Commun.* **6**, 1 (2015).
- [69] F. S. Piccioli, A. Szameit, and I. Carusotto, Topologically protected frequency control of broadband signals in dynamically modulated waveguide arrays, *Phys. Rev. A* **105**, 053519 (2022).